Histol Histopathol (2020) 35: 1151-1157

http://www.hh.um.es

Histology and Histopathology
From Cell Biology to Tissue Engineering

Genetic investigation of nodal melanocytic nevi in cases of giant congenital melanocytic nevus

Y. Cao[1], X. Yang[2], Y.-M. Lai[2], L. Jia[2], X.-T. Diao[2], Q. Zhuang[1] and D.-M. Lin[2]

[1]Department of Pathology, Plastic Surgery Hospital, Chinese Academy of Medical Sciences and Peking Union Medical College, Beijing, China and [2]Department of Pathology, Key Laboratory of Carcinogenesis and Translational Research (Ministry of Education), Peking University Cancer Hospital and Institute, Beijing, China

Summary. Nodal melanocytic nevi are common incidental findings in lymph nodes that have been removed during sentinel lymph node biopsy for melanoma. They can also occur in the local lymph nodes of the giant congenital nevus (GCN), but very little is known regarding nodal melanocytic nevi in the giant congenital nevus, especially at the genetic level. There are two theories that explain the possible pathogenesis of nodal melanocytic nevi, mechanical transport and arrested migration during embryogenesis. However, there have been few tests of these two theories at the molecular biology level until now. We used whole-exon sequencing to test these two theories at the gene level for the first time.

In clonal evolution analysis of patient 1, whose tumor mutation burden (TMB) value was relatively stable, showed that the GCN and nodal nevus had the same initial origin and then diverged into two branches as a result of gene mutations. In contrast, analysis indicated that in the other patient, whose TMB value declined from 68.02/Mb in a GCN to 17.55/Mb in associated nodal nevi, these two samples were from different origins at the beginning, each with its own gene mutation. These results are consistent with the two respective theories at the molecular biological level.

We provided the first tests of the two theories of pathogenesis of nodal melanocytic nevi at the gene level, and these findings may provide some clues for further study. In addition, not all nodal nevi should be treated as lymph node metastasis in clinical diagnosis, and we should make a comprehensive assessment and judgment of nodal melanocytic nevi based on morphology, immunological characteristics and fluorescence in situ hybridization (FISH) tests.

Key words: Giant congenital nevus, Nodal melanocytic nevi, Whole-exon sequencing, Prognosis, Theories

Offprint requests to: Prof Dongmei Lin, Department of Pathology, Key Laboratory of Carcinogenesis and Translational Research (Ministry of Education), Peking University Cancer Hospital and Institute, NO. 52 Fucheng Rd, Haidian District, Beijing, 100142, PR China. e-mail: lindm3@163.com

DOI: 10.14670/HH-18-243

Introduction

Nodal melanocytic nevi predominantly form compact focal aggregates in the fibrous capsules and trabeculae of lymph nodes and have also been described in the nodal parenchyma and sinusoids (Biddle et al., 2003). Melanocytic lymph node deposits are common incidental findings in lymph nodes removed during sentinel lymph node biopsy for melanoma. These nodal melanocytic nevi, or melanocytic rests, are estimated to occur in 3-22% of lymph nodes from melanoma patients (Bowen et al., 2015). Furthermore, nodal melanocytic nevi can also occur in the local lymph nodes of a congenital giant nevus (GCN) (Hara, 1993; Bowen et al., 2015). The lymph node nevus in a case of congenital nevus may be difficult to diagnose and may be mistaken for malignant transformation of nevus with lymph node metastasis from a diagnostic standpoint. However, most of the current literature addresses the study of nodal nevi in melanoma, while it is sparse with regard to the histopathology of lymph nodes associated with giant congenital melanocytic nevi. Therefore, it is necessary to

further investigate nodal nevi which are related to congenital melanocytic nevi, especially at the gene level.

The mechanism by which melanocytes are transported to lymph nodes is still unclear. Prevailing theories include lymphatic transfer of melanocytes from a cutaneous nevus to a lymph node in the lymphatic drainage basin and an embryologic phenomenon whereby neural crest-derived melanocytes are transported to lymph nodes during in utero migration (Carson et al., 1996; Holt et al., 2004). However, there have been few studies of these two potential mechanisms at the molecular biological level. Our study filled this gap and used the method of whole-exon sequencing to verify these two theories at the gene level for the first time. Additionally, efforts to explain the mechanisms of melanocyte transport to lymph nodes may contribute to understanding the metastatic process.

Materials and methods

Patients and sample selection

Of the more than 7000 patients diagnosed with congenital melanocytic nevus in our department over the past 10 years, only 2 had GCN with nodal nevi. Formalin-fixed and paraffin-embedded (FFPE) tissue specimens (both GCN and nodal nevi) of these 2 cases were collected retrospectively, and paired normal skin was also collected. The key clinical and pathological characters of the patients are presented in Table 1 and Fig. 1.

Cytogenetic analysis

DNA extraction from FFPE samples

Tumor cells and paired normal cells were scraped and collected in 10-μm thick formalin-fixed paraffin-embedded (FFPE) sections for each histological lesion from the two cases. The tumor content was estimated by pathologists to ensure more than 90% of cells were tumor cells. More than ten sections of each FFPE sample were collected to ensure adequate DNA would be extracted. DNA was isolated from the FFPE samples using the DNeasy Blood and Tissue Kit (69504, QIAGEN, Venlo, Netherlands), according to the manufacturer's instructions.

Whole-exome sequencing (WES)

WES was carried out using the technique of next-generation sequencing (NGS) in order to detect the genomic alterations of those tissue specimens. The main procedures were as follows:

DNA quality control. The quantity of purified DNA was assessed by fluorometry (Qubit 3.0, Thermo Fisher). The concentration of the purified DNA needs to be greater

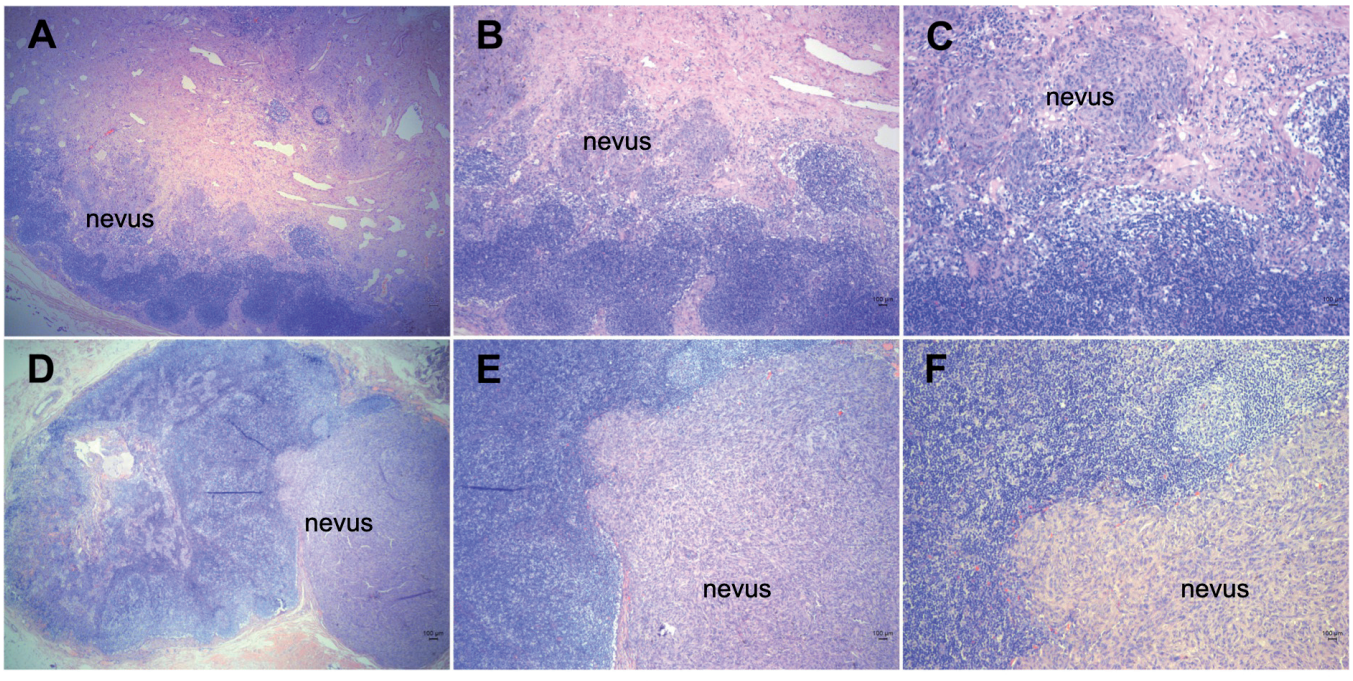

Fig. 1. Melanocytic cells were arranged as small nests and cords, mainly in the subcapsular of lymph nodes. The nuclei of the melanocytic cells showed no nuclear dysplasia. No mitosis or necrosis was evident. Patient 1 **(A-C)**, Patient 2 **(D-F)**.

than 1 ng/ul, and total quantity must meet the standard of over 40 ng. The quality of purified DNA was evaluated via gel electrophoresis. Highly degraded DNA with most fragments shorter than 200 bp may lead to the failure of library construction.

Library construction. We first created targeted capture pulldown using the Capture system (IDT xGen®Exome). After hybridization, captured targets were condensed, and selected regions were then amplified via PCR. Exon-wide libraries from native DNA were generated using the TruePrep DNA Library Prep Kit V2 for Illumina (#TD501, Vazyme, Nanjing, China). Libraries were subsequently quantified using a Qubit dsDNA HS Assay kit (Thermo Fisher), following the manufacturer's protocols. Before sequencing, constructed libraries met the following standards: concentration ≥1 ng/uL, total quantity ≥5 ng, and the lengths of fragments were mainly 150 bp-250 bp (Agilent2100 analyzer).

Sequencing. Paired-end sequence data were then created using Illumina HiSeq machines. The Exome Research Panel - Integrated DNA system (Tongshu BioTech, Shanghai, China) was used to accomplish WES. Average sequencing depth of coverage was greater than 250×, and more than 99% of exons had sequencing depth of >100×.

Sequencing quality control. The quality of reads was examined using FastQC to assess baseline quality characteristics, such as sequence quality scores, GC content, N content. Linkers and primers were removed afterwards. After assessing the quality of reads, low-quality bases below Q20 were trimmed.

Sequence alignment. The sequence data were first aligned to the human reference genome (NCBI build 37) using BWA (Slater et al., 2009) and then sorted by the sambamba package to mark duplicates (Tarasov et al., 2015).

Variant call and annotation. Germline mutations were analyzed by HaplotypeCaller (Poplin et al., 2017), using data in a BAM file generated from sambamba, removing replicants. Germline mutations in each sample were annotated with ANNOVAR afterwards, and the annotated files were converted to an MAF file using maftools, as were somatic mutations.

Somatic mutation calling was further performed using VarDict (Lai et al., 2016). To calculate TMB, somatic mutations in each patients' samples were annotated with ANNOVAR (Wang et al., 2010), and the annotated files were converted to an MAF file using maftools (Mayakonda et al., 2018). After removing synonymous mutations, the number of nonsynonymous mutations for each sample was divided by the size of the WES probe panel (Mb) to obtain the value of TMB (/Mb).

Phylogenetic trees. The clonal evolution process was analyzed for these two cases. In brief, after obtaining data for somatic mutations, CNV and LOH as previously mentioned, the number of bases for each allele was counted using bam-readcount, available online: https://github.com/genome/bam-readcount, to calculate variant allele frequency (VAF). Subclonal architecture analysis was performed afterwards with sciClone (Miller et al., 2014), using the VAF, CNV and LOH data. Clustering results were imported into clonevol to construct evolutionary trees (Dang et al., 2017).

Statistical analysis. Clinicopathological features of the patients examined in our study were collected. Non-normally distributed data were analyzed by Wilcoxon's rank sum test. Statistical analysis was carried out by the ggpubr package. All tests were two-tailed, with $p<0.05$ indicating significant difference.

Fluorescence in situ hybridization (FISH)

We also tested four samples (G1-N, G1-L, G2-N, G2-L) with fluorescence in situ hybridization (FISH). Analysis with probes targeting 6p25 (RREB1), centromere6, 6q23 (MYB), and 11q13 (CCND1) (Abbott Bio. Ltd.) was accomplished as previously described (Gerami et al., 2009). Signals were scored according to previously determined criteria and thresholds. The results were considered to be positive if 55% or more nuclei had higher RREB1 signal counts than Cep6 signal counts, if 40% of nuclei had lower

Table 1. Clinical and pathological characteristics of the two patients.

	Patient 1		Patient 2	
Diagnosis	GCN with nodal nevi		GCN with nodal nevi	
sex	F		F	
age	23		2	
Clinical detail	GCN with nodal nevi on the head		GCN with nodal nevi on the head and neck	
Microscopy (Fig.1)	Melanocytic cells were arranged as small nests and cords, mainly in the subcapsular of lymph node. The nuclei of the melanocytic cells showed no nuclear dysplasia. No mitosis or necrosis is evident. The morphology of nevus cells is similar to that of nevus cells in GCN.			
Outcome	Alive, 75monthes after diagnosis		Alive, 96monthes after diagnosis	
Sample numbers	G1-N	G1-L	G2-N	G2-L
Tissues for genetic investigation	GCN, Lt head	Nodal nevi, Lt head	GCN, Lt head	Nodal nevi, Lt head

MYB signal counts than Cep6, if 29% or more nuclei had >2 signals for RREB1, or if 38% or more nuclei had >2 signals for CCND1 (Gerami et al., 2009).

Results

Tumor mutation burden (TMB)

It is worthwhile to note that TMB value declined from 68.02/Mb in cutaneous GCN to 17.55/Mb in associated lymph node nevi of patient 2. However, TMB values were fairly similar in different samples (3.45/Mb in cutaneous GCN vs 4.78/Mb in lymph node nevi) of patient 1 (Fig. 2).

Somatic driver mutations and copy number variations

A total of 3,712 somatic coding mutations and 2,991 copy number variations were detected among 5,181 genes. The driver genes altered in at least two samples are presented in Fig. 3. For patient 1, amplifications of *SCRIB, DEPTOR* and *MYC,* as well as mutations in CIR1, occurred in both cutaneous GCN and lymph node nevi. For patient 2, both cutaneous GCN and lymph node nevi harbored mutations in *AXIN2, CTCF, FAT1, GTF2I, PBRM1, PIK3CG* and *SETBP1*. Mutations in GNAQ were specific to the GCN, and mutations in KMT2B were specific to lymph node nevi. Alteration in NRAS was only detected in lymph node nevi of patient 2.

Clonal evolution analysis

The clonal evolution process was analyzed for these two cases. Fig. 4A,C depict the subclonal architecture and clonal evolution tree of patient NO.1 with lymph node nevi. Fig. 4B,D display the same for patient NO.2. In NO.1, melanocytes from lymph node tissue did not form an independent cluster while those from the primary GCN did. In contrast, the primary GCN and associated lymph node nevi derived from one cluster and evolved into two branches shortly thereafter in NO.2.

FISH test

The results of the FISH test were negative for all samples (Table 2), and some results of G1-L and G2-L are shown in Fig. 5.

Discussion

Nodal melanocytic nevus is a common incidental finding among lymph nodes removed during sentinel lymph node biopsy for melanoma (Bowen et al., 2015)

Table 2. All samples demonstrated negative in FISH test.

Sample number	G1-N	G1-L	G2-N	G2-L
Proportion of tumor cells with CCDN1 signal counts > 2	6.70%	6.70%	13.30%	6.70%
Proportion of tumor cells with RREB1 signal counts > 2	10.00%	3.30%	16.70%	10.00%
Proportion of tumor cells with RREB1 signal counts >CEP6	3.30%	6.70%	10.00%	3.30%
Proportion of tumor cells with MYB signal ncounts <CEP6	6.70%	10.00%	6.70%	6.70%
The result of FISH	-	-	-	-

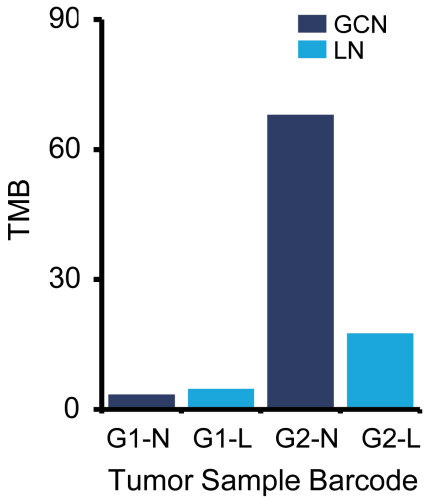

Fig. 2. The TMB values of the four samples.

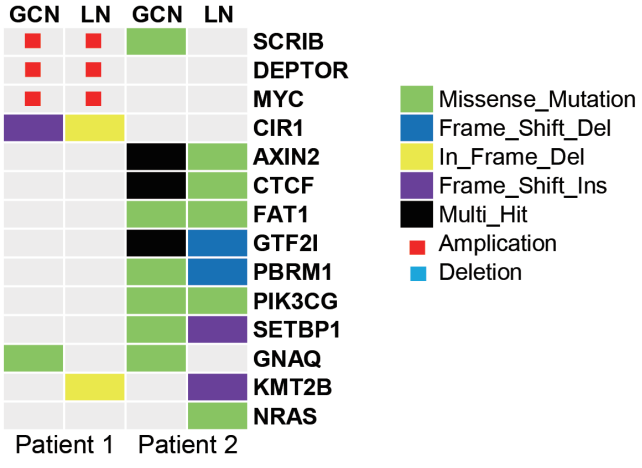

Fig. 3. The altered driver genes in each sample.

and can also be detected in cases of GCN. A misdiagnosis of melanoma metastasis as nodal melanocytic nevus may lead to inappropriate treatment. Therefore, it is important to reveal the pathogenesis under this phenomenon.

A manufactured FISH test with probes targeting 6p25 (RREB1), 6q23 (MYB), Cep6 and 11q13 (Cyclin D1) is widely applied in diagnosis and differential diagnosis of melanoma. This test has high sensitivity and specificity in distinguishing malignant melanoma from benign melanocytic nevi, based on the nonoverlapping patterns of chromosomal aberrations of these two tissues (Gerami et al., 2009; de Klein et al., 2012). It is widely used in the diagnosis of melanoma. In our research, four samples all tested negative via FISH, and we could infer these nodal nevi were similar to cutaneous GCN and were benign melanocytic nevi. All these results are consistent with previous findings that nevus cell aggregates in lymph nodes should be considered a benign condition (Holt et al., 2004; Gambichler et al., 2013), while in patients with melanoma the rates of distant recurrence and overall survival are similar in patients with nodal nevus to those rates in patients who do not have metastatic melanoma (Smith et al., 2016;

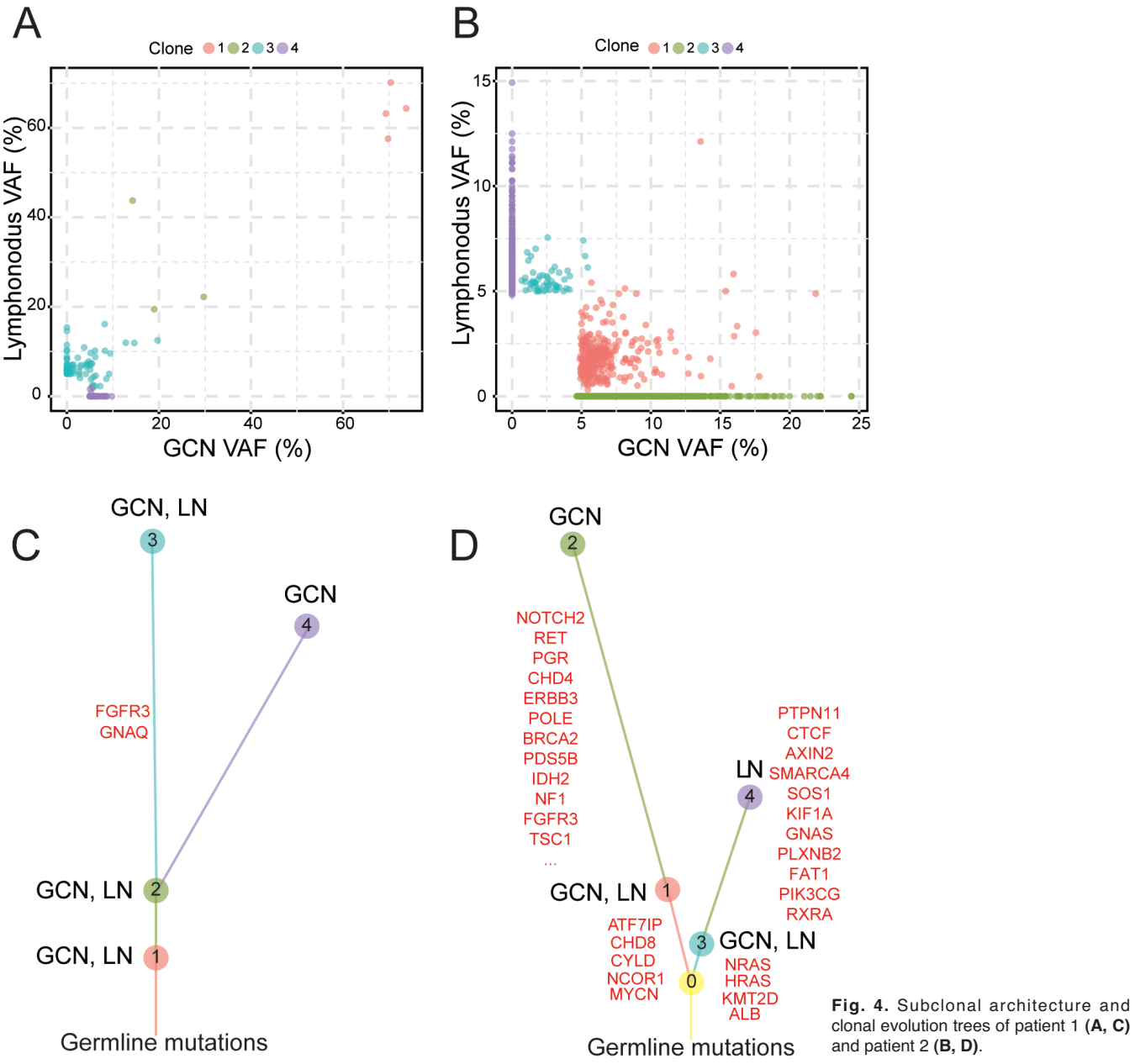

Fig. 4. Subclonal architecture and clonal evolution trees of patient 1 **(A, C)** and patient 2 **(B, D)**.

Kim et al., 2018; Lezcano et al., 2020).

Therefore, when we encounter GCN in clinical practice, it cannot be completely determined that congenital nevus involves malignant transformation accompanied by lymph node metastasis. We should make a comprehensive assessment and judgment from the aspects of morphology, immunological characteristics and FISH about any nodal melanocytic nevus.

In these two cases in our study, the NRAS mutations that were most common in giant nevi occurred only in nodal nevi in patient 2. Few driver alterations in GCN or nodal nevi were shared by the two patients. GCN and nodal nevus in the same patient harbored more shared altered driver genes. Compared with patient 1, GCN and nodal nevus in patient 2, which may have different origins, seemed to have a greater number of common mutated driver genes. However, most of these driver genes had different mutations. More cases are necessary to identify the genetic differences and commonalities between GCN and nodal nevus.

There have been two prevailing theories of nodal melanocytic nevus pathogenesis; one is known as benign metastasis describing the pathogenesis as mechanical transport of melanocytes, the other one involves arrested migration assuming melanocyte deposition during embryogenesis (Patterson, 2004). However, to our knowledge, the underlying genetic changes of melanocytes in lymph nodes remained unclarified, and both embryologic and mechanical transport hypotheses have been postulated. Our comparative genomic analysis illuminated the genetic alterations of this specular phenomenon in GCN, and the results corresponded to these two respective theories.

In our research, the clonal evolution analysis of patient 1 showed that the cutaneous GCN and nodal nevus had the same origin initially, and then diverged into two branches with gene mutations. One continued in the cutaneous GCN and the other terminated in both nodal nevi and GCN. In addition, the TMB values were relatively stable in different samples (3.45/Mb in GCN vs 4.78/Mb in nodal nevi), and this might further suggest that the two samples may have the same origin. These gene-level results are consistent with the mechanical transport hypothesis that nodal nevi are produced by lymphatic transfer of melanocytes from a cutaneous nevus to a lymph node in the lymphatic drainage basin (Hara, 1993).

In our study, the clone analysis for patient 2 clearly showed that these two samples were from different initial origins, each with its own gene mutation without mutual influence. In addition, it is worthwhile to note that the TMB value declined from 68.02/Mb in the primary GCN to 17.55/Mb in associated nodal nevi. It is assumed that lymph node deposition may have occurred early, as the genes in cutaneous GCN continued mutating while melanocytes transported to lymph nodes were arrested. Furthermore, the nodal nevus was detected in the first surgery of patient 2 when she was 2 years old, which makes it more likely to have occurred during the embryonic period. All of the above findings support the hypothesis of lymph node arrest, under which nodal melanocytic deposition happened during embryogenesis (Patterson, 2004).

We have confirmed these two theories at the gene level for the first time; however, due to the small number of samples, our results do not indicate which mechanism is more frequent. From our study, however, we may infer that the younger the patients are, the more likely they are to form nodal nevi during embryonic development;

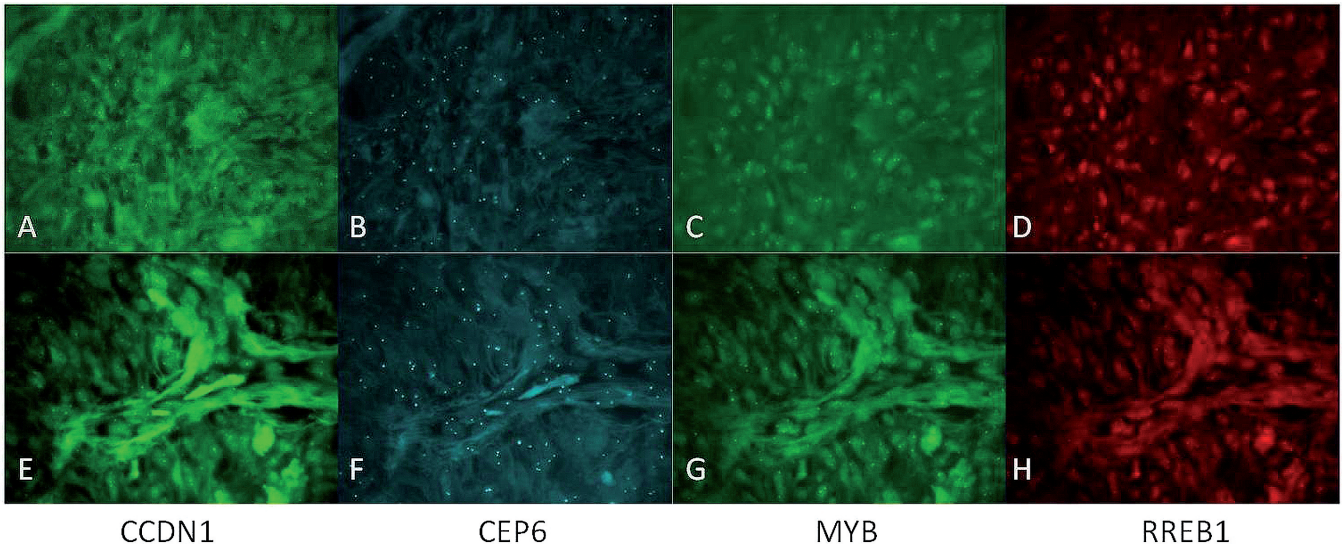

Fig. 5. The results of FISH in samples G1-L **(A-D)** and G2-L **(E-H)**.

further, the later the lymph node nevus has developed, the more likely it is that the underlying mechanism was lymph drainage. These two theories need further research and confirmation.

Conflicts of Interest. This study did not receive any funding. All authors declare that there was no conflict of either financial or non-financial interests.

References

Biddle D.A., Evans H.L., Kemp B.L., El-Naggar A.K., Harvell J.D., White W.L., Iskandar S.S. and Prieto V.G. (2003). Intraparenchymal nevus cell aggregates in lymph nodes: a possible diagnostic pitfall with malignant melanoma and carcinoma. Am. J. Surg. Pathol. 27, 673-681.

Bowen A.R., Duffy K.L., Clayton F.C., Andtbacka R.H. and Florell S.R. (2015). Benign melanocytic lymph node deposits in the setting of giant congenital melanocytic nevi: the large congenital nodal nevus. J. Cutan. Pathol. 42, 832-839.

Carson K.F., Wen D.R., Li P.X., Lana A.M., Bailly C., Morton D.L. and Cochran A.J. (1996). Nodal nevi and cutaneous melanomas. Am. J. Surg. Pathol. 20, 834-840.

Dang H.X., White B.S., Foltz S.M., Miller C.A., Luo J., Fields R.C. and Maher C.A. (2017). ClonEvol: clonal ordering and visualization in cancer sequencing. Ann. Oncol. 28, 3076-3082.

de Klein A., Koopmans A.E. and Kilic E. (2012). Multicolor FISH with improved sensitivity and specificity in the diagnosis of malignant melanoma. Expert Rev. Mol. Diagn. 12, 683-685.

Gambichler T., Scholl L., Stucker M., Bechara F.G., Hoffmann K., Altmeyer P. and Othlinghaus N. (2013). Clinical characteristics and survival data of melanoma patients with nevus cell aggregates within sentinel lymph nodes. Am. J. Clin. Pathol. 139, 566-573.

Gerami P., Jewell S.S., Morrison L.E., Blondin B., Schulz J., Ruffalo T., Matushek P.t., Legator M., Jacobson K., Dalton S.R., Charzan S., Kolaitis N.A., Guitart J., Lertsbarapa T., Boone S., LeBoit P.E. and Bastian B.C. (2009). Fluorescence in situ hybridization (FISH) as an ancillary diagnostic tool in the diagnosis of melanoma. Am. J. Surg. Pathol. 33, 1146-1156.

Hara K. (1993). Melanocytic lesions in lymph nodes associated with congenital naevus. Histopathology 23, 445-451.

Holt J.B., Sangueza O.P., Levine E.A., Shen P., Bergman S., Geisinger K.R., and Creager A.J. (2004). Nodal melanocytic nevi in sentinel lymph nodes. Correlation with melanoma-associated cutaneous nevi. Am. J. Clin. Pathol. 121, 58-63.

Kim H.J., Seo J.W., Roh M.S., Lee J.H. and Song K.H. (2018). Clinical features and prognosis of Asian patients with acral lentiginous melanoma who have nodal nevi in their sentinel lymph node biopsy specimen. J. Am. Acad. Dermatol. 79, 706-713.

Lai Z., Markovets A., Ahdesmaki M., Chapman B., Hofmann O., McEwen R., Johnson J., Dougherty B., Barrett J.C. and Dry J.R. (2016). VarDict: a novel and versatile variant caller for next-generation sequencing in cancer research. Nucleic Acids Res. 44, e108.

Lezcano C., Pulitzer M., Moy A.P., Hollmann T.J., Jungbluth A.A. and Busam K.J. (2020). Immunohistochemistry for PRAME in the distinction of nodal nevi from metastatic melanoma. Am. J. Surg. Pathol. 44, 503-508.

Mayakonda A., Lin D.C., Assenov Y., Plass C. and Koeffler H.P. (2018). Maftools: efficient and comprehensive analysis of somatic variants in cancer. Genome Res. 28, 1747-1756.

Miller C.A., White B.S., Dees N.D., Griffith M., Welch J.S., Griffith O.L., Vij R., Tomasson M.H., Graubert T.A., Walter M.J., Ellis M.J., Schierding W., DiPersio J.F., Ley T.J., Mardis E.R., Wilson R.K. and Ding L. (2014). SciClone: inferring clonal architecture and tracking the spatial and temporal patterns of tumor evolution. PLoS Comput. Biol. 10, e1003665.

Patterson J.W. (2004). Nevus cell aggregates in lymph nodes. Am. J. Clin. Pathol. 121, 13-15.

Poplin R., Ruano-Rubio V., DePristo M.K., Fennel T.J., Carneiro M.O., Van der Auwera G.A., Kling D.E., Gauthier L.D., Levy-Moonshine A., Roazen D., Shakir K., Thibault J., Chandran S., Whelan C., Lek M., Gabriel S., Daly M.J., Neale B., MacArthur D.G. and Banks E. (2017). Scaling accurate genetic variant discovery to tens of thousands of samples. bioRxiv. doi: https://doi.org/10.1101/201178, 1-22.

Slater P.M., Grivell R. and Cyna A.M. (2009). Labour management of a woman with carnitine palmitoyl transferase type 2 deficiency. Anaesth. Intensive Care 37, 305-308.

Smith O.J., Coelho J.A., Trevatt A.E. and Ross G.L. (2016). Clinical significance of intra-nodal naevi in sentinel node biopsies for malignant melanoma. Eur. J. Surg. Oncol. 42, 1427-1431.

Tarasov A., Vilella A.J., Cuppen E., Nijman I.J. and Prins P. (2015). Sambamba: fast processing of NGS alignment formats. Bioinformatics 31, 2032-2034.

Wang K., Li M. and Hakonarson H. (2010). Analysing biological pathways in genome-wide association studies. Nat. Rev. Genet. 11, 843-854.

Accepted July 30, 2020